



NLR-TP-2001-208

**Computational model for electromagnetic  
interaction of conformal antennas and  
aircraft structure**

H. Schippers, J. Verpoorte and G. Vos



NLR-TP-2001-208

## **Computational model for electromagnetic interaction of conformal antennas and aircraft structure**

H. Schippers, J. Verpoorte and G. Vos

This investigation has been carried out under a contract awarded by the Ministry of Defence, contract number 726.97.0357.01.

The Ministry of Defence has granted NLR permission to publish this report.

This report is based on a presentation held at the 2<sup>nd</sup> European Workshop on Conformal Antennas, 24 and 25 April 2001, The Hague, The Netherlands.

The contents of this report may be cited on condition that full credit is given to NLR and the authors.

Division:	Avionics
Issued:	22 May 2001
Classification of title:	Unclassified



## Contents

I.	INTRODUCTION	3
II.	COMPUTATIONAL MODEL	3
III.	CONFORMAL ARRAY ON GENERIC AIRCRAFT	5
IV.	SAR ANTENNA ON FIGHTER AIRCRAFT	5
V.	CONCLUSIONS AND RECOMMENDATIONS	5
VI.	ACKNOWLEDGEMENTS	5
VII.	REFERENCES	5

8 Figures

(6 pages in total)



# Computational Model for Electromagnetic Interaction of Conformal Antennas and Aircraft Structure

H. Schippers<sup>NLR</sup>, J. Verpoorte<sup>NLR</sup>, G. Vos<sup>NLR</sup>

**Abstract**—The aim of this paper is to describe a computational model for assessment of electromagnetic interaction of conformal antennas with the aircraft structure. The conformal array antennas are assumed to be flush-mounted on the surface of an aircraft. The model assumes a receiving conformal antenna, which is illuminated by a plane wave. The electromagnetic field that is scattered by the aircraft (itself) on the antenna is taken into account. The mathematical modeling of the electromagnetic field is divided into two parts. The first part is concerned with the modeling of the scattered field in the region outside the aircraft, the second part is related to the modeling of the electromagnetic properties of the array elements. The computational model is applied to a conformal array antenna (consisting of 16 microstrip patch antennas) on a generic aircraft and a generic phased array antenna on a pod of a fighter aircraft. The numerical results of the generic aircraft are compared with measurements that have been carried out on NLR's Antenna Test Range.

## I. INTRODUCTION

Smart skin array technology is being developed aiming at improvement of aircraft performance and systems capabilities. Sensors, signal processors, signal and power distribution networks and associated control functions are integrated with a composite load-bearing skin structure to form an interface with the flight environment. Smart skin antennas can be classified as active phased array antennas of the conformal type using transmit/receive modules, which are constructed in the form of thin flat layers. Smart skin antennas are especially suited for application to aircraft where they are flush-mounted to the exterior of the vehicle. Smart skin array technology provides almost hemispherical coverage by the antenna beam, which is not possible presently with a flat plate array antenna in the nose of the aircraft.

In this report a computational model is described to analyze the effects of the aircraft structure on radiation characteristics of a conformal array antenna which is flush-mounted on the surface of the aircraft. It is assumed that the aircraft is illuminated by a plane wave. The disturbance of the radiation pattern of the array antenna is predicted by means of a hybrid approach. High-frequency approximations based on physical and geometrical optics are used to predict the total electric field incident at the

surface of the array. The total field follows from superposing the incident and scattered field by the aircraft itself (see figure 1). The antenna consists of an array of microstrip patch elements, which are mounted on a supporting structure (see figure 2). The total incident electric field at the surface of the array is used to compute the induced voltage at the patch elements. The characteristics of the microstrip patches are represented by means of magnetic fringe currents at radiating/receiving slots and the Transmission Line Model (see Ref [1]). As a result an expression is obtained for the induced currents on the coaxial feeds of the patches, which can be combined in case of an array antenna.

The outline of the paper is as follows. In section II the computational modeling is described. In section III the model is applied to a conformal array antenna (consisting of 16 patches) on a generic aircraft. The numerical results are compared with measurements that have been carried out on NLR's Antenna Test Range. In section IV the model is applied to a generic "Synthetic Aperture Radar" antenna mounted on a pod of a fighter aircraft. Conclusions and recommendations are presented in section V.

## II. COMPUTATIONAL MODEL

The conformal array antenna is mounted on the surface of the aircraft. The aircraft is assumed to be perfectly electric conducting. The patches of the conformal array antenna are on a dielectric substrate.

It is assumed that the aircraft is illuminated by a plane wave (with direction vector  $\hat{k}^i$ ). With the incident plane wave an electric field is associated with direction  $\hat{e}^i$  and magnitude  $E_0$ . The electric and magnetic fields are specified as:

$$\vec{E}^i = \hat{e}^i E_0 e^{-jk^i \cdot \vec{r}} \quad , \quad \vec{H}^i = \hat{k}^i \times \vec{E}^i / \eta \quad , \quad (1)$$

with  $\eta$  the impedance of free space. Furthermore,  $k$  is the wave number given by  $k = 2\pi / \lambda$ , with  $\lambda$  the wavelength of the incident field.

The objective of the computational model is to predict the induced currents of the coaxial feed probes which are connected to the patches, where the electromagnetic field that is scattered by the aircraft (itself) on the antenna is taken into account (see figure 1). The mathematical modeling of the electromagnetic field is divided into two



parts. The first part is concerned with the modeling of the scattered field in the region outside the aircraft that is occupied by the air, the second part is related to the modeling of the electromagnetic fields in the substrate of the patches. The first domain is relative large with respect to the wavelength of the incident field, while the second domain is small. Therefore, the electromagnetic field in the first domain is determined by means of approximate high-frequency methods based on physical and geometrical optics. The array antennas, which have been used for the measurements, consist of a collection of simple patch antennas, which are mounted on a supporting structure. Each patch has its own substrate. By means of measurements a weak coupling has been observed between the patch antenna elements. Therefore, an approximate model for the propagation of waves in the patch antennas is sufficient (instead of a full wave model). In the present computational model each microstrip patch antenna patch is represented by means of two parallel slots with magnetic fringe fields connected by a transmission line.

#### A. High frequency approximations

The total electromagnetic field in the domain outside the scattering object is written as the sum of the incident field and the scattered field,

$$\vec{E}^T = \vec{E}^i + \vec{E}^S, \quad \vec{H}^T = \vec{H}^i + \vec{H}^S. \quad (2)$$

The scattered field due to multipath reflections follows from far field expressions (see Ref. [2], p. 88) of the Stratton-Chu integral representations. The scattered electric field reads

$$\vec{E}^S(\vec{r}) = -jk\eta \frac{e^{-jkR}}{4\pi R} \int_S \left\{ \vec{J} - \hat{R} \cdot \vec{J} \hat{R} + \frac{1}{\eta} \vec{M} \times \hat{R} \right\} e^{jk_0 \vec{r} \cdot \hat{R}} dS \quad (3)$$

A similar formula holds for  $\vec{H}^S$ . Here,  $R$  is the distance from the origin to the observation point ( $R = |\vec{r}|$ ) and  $\hat{R}$  is the unit vector from the origin to the observation point, i.e.  $\hat{R} = \vec{r}/R$ . The integral expressions for the scattered field still contain the unknown surface current distributions  $\vec{J}$  and  $\vec{M}$ . Since the aircraft is assumed to be perfectly electric conducting, it follows that  $\vec{M} = 0$ , and  $\vec{J} = 2\hat{n} \times \vec{H}^i$  on illuminated parts of the aircraft. On non-illuminated parts  $\vec{J}$  is also put equal to zero. Geometrical Optics and ray tracing are applied to determine the illuminated parts and the local incident fields.

The following procedure is followed:

**-1-** The exterior surface of the aircraft is geometrically approximated by a collection of triangular panels with reflection coefficients according to perfectly conducting surfaces (see figure 3); **-2-** the aircraft is illuminated by an incident plane wave according to equation (1). The triangular panels that are illuminated, either directly by the incident wave or indirectly by a multiple reflected wave, are

determined by means of ray-tracing algorithms. Rays are fired from the corner points of the triangular panels towards the source of the electromagnetic radiation (i.e. in the direction  $-\hat{k}^i$ ). If the rays are not blocked by any part of the object, the whole panel is illuminated. Otherwise, the shadowed part is determined. The reflected field is determined by applying Snell's laws of Geometrical Optics. When the reflected field hits the object again, this field is used as incident field to calculate the contribution to the second reflection. This procedure can be repeated until there are no reflections left. **-3-** The electric surface currents  $\vec{J}$  on the illuminated panels are approximated by Physical Optics (PO) currents using the reflected fields as incident fields; on the shadowed panels the surface currents are set to zero. **-4-** The scattered fields at the slots of the patch elements are computed by means of equation (3).

#### B. Patch model with magnetic fringe fields

The microstrip radiator element may be treated as a line resonator with no transverse field variations. The fields vary along the length, which is usually half a wavelength and the radiation occurs mainly from the fringing fields at the open-circuited ends (see Ref. 1 pp. 48). The microstrip patch element may be represented as two slots spaced a distance  $L$  apart. Each slot radiates the same field as a magnetic dipole with magnetic current of:

$$\vec{M} = \frac{2V}{h} \vec{m}, \quad (4)$$

where the factor 2 arises due to the positive image of  $\vec{M}$ , which is near the ground-plane, and  $V$  is the voltage across the slot. The vector  $\vec{m}$  is the unit direction vector of the magnetic surface current. The total electric field due to the magnetic current  $\vec{M}$  in equation (4) on the surface of the slots can then be approximated by:

$$\vec{E}(\vec{r}) = -jk \frac{e^{-jkR}}{4\pi R} \int_S \vec{M}(\vec{r}) \times \hat{R} e^{jk_0 \vec{r} \cdot \hat{R}} dS \quad (5)$$

The direction vector  $\hat{R}$  equals the opposite of the direction of the incident field (direct or indirect field). According to the principal of reciprocity the receiving characteristics of the slot can be computed from equations (4) and (5) by

$$V(\vec{r}) = \frac{h}{2jk} \int_S e^{jk_0 \vec{r} \cdot \hat{k}^i} dS \vec{m}(\vec{r}) \times \hat{R} \cdot \vec{E}(\vec{r}), \quad (6)$$

with  $\vec{E}$  the total electric field that is received at the slot. This field follows from equation (2).

By means of the "Transmission line model" (see Ref [1], page 48), the voltages on the radiating slots are combined to a voltage on each antenna element and the array pattern can be constructed with respect to the magnitude and phase of the voltages on the antenna elements.



### III. CONFORMAL ARRAY ON GENERIC AIRCRAFT

The generic aircraft is defined as a cylinder mounted via a pylon on a flat plate of size 2m x 2m (see figure 4). On the cylinder, 16 microstrip patch antennas are mounted as a conformal array of 4 by 4 elements. The metal surface of the generic aircraft has been made of aluminium. In the length direction of the cylinder, the elements of the conformal antenna can be considered as a planar array of patch elements. However across the surface of the cylinder, the antenna is faceted according to the curved surface of the cylinder. The antenna array elements have been constructed on a separate wedge-shaped structure (see Figure 2). The patch elements have been designed for a frequency of 1811 MHz. (wavelength  $\lambda$  measures 0.165m). All patch elements are excited equally in amplitude, however the edge rows are excited with a phase lag of  $85^\circ$  compared to middle two rows. This phase shift results in a main-beam steered in the direction parallel to the wing and perpendicular to the cylinder axis.

Results of computations and measurements of this conformal array on the generic aircraft are displayed in figures 5 and 6 for both polarization directions. The correlation between the measurements and the calculations appears satisfactory. A good correlation is observed for the locations of the local minimum values (nulls) and the local maximum values (peaks) of the output power. However the value of the peaks and nulls differ slightly. Furthermore, the abrupt decrease of the calculated pattern for  $\phi \approx -25^\circ$  is due to blocking of all array elements by the edge of the wing. This effect and the other discrepancies between the calculated and measured patterns will be corrected for by a future extension of the computational model with modeling of edge-diffraction.

### IV. SAR ANTENNA ON FIGHTER AIRCRAFT

For demonstration of the computational model a generic Synthetic Aperture Radar (SAR) has been designed on a pod of a fighter aircraft (see figure 7). SAR applications are employed on both aircraft and spacecraft for earth-observation. They require in general highly directional antennas with low side-lobe levels. Any error in the main beam direction, beam-width or an increase of the side-lobe levels caused by electromagnetic interaction with the aircraft will have a significant effect on the final image produced by the SAR. The antenna consists of a faceted two-dimensional array of patch antennas. Across-track the array consists of 23 patch antenna elements conformal to the surface. The length of the array along-track contains 30 patch antenna elements (see Figure 7). The antenna has been designed at frequency of 5.3 GHz.

The co-ordinate system of the aircraft was defined as shown in figure 3. The flight direction is along the minus X-axis and the direction of the star-board wing is related to the Y-axis. The Z-axis is directed towards zenith. The main beam direction of the SAR antenna is chosen in the direction of the Y-axis ( $\theta = 90^\circ$ ,  $\phi = 90^\circ$ ) to show the effect of the aircraft.

Figure 8 shows the computational results of the radiation pattern of the SAR antenna mounted on the pod, compared to the theoretical results of the SAR antenna without the interaction of the surrounding aircraft. It is observed that the radiation patterns of the installed antenna differ from the theoretical design for several angles of incidence. For an observation point of  $\theta = 170^\circ$ , a major increase of the side-lobe level is observed. For these angles not only the incident field contributes to the receiver, but also the reflected fields from the pylon tanks.

### V. CONCLUSIONS AND RECOMMENDATIONS

A hybrid computational model has been described for the electromagnetic interaction of the conformal array antenna on the aircraft with the aircraft structure. The multipath effects have been taken into account by modeling the electromagnetic field exterior to the aircraft by high frequency approximations. The characteristics of the elements of the array antenna have been represented by means of magnetic fringe currents at radiating/receiving slots of the microstrip patches. The output of each array element was calculated by using a transmission line model. The hybrid method has been validated by a comparison of numerical results and measurement data. The comparison reveals that this hybrid method provides satisfactory accurate results. However, to enable the evaluation of future antenna installations without prior flight tests or measurements on scale models, it is recommended to extend the computational approach with modeling of edge diffraction. Then, the computational model can be used well to predict the actual performance of conformal array antennas on aircraft and other vehicles.

### VI. ACKNOWLEDGEMENTS

This investigation has been carried out partly under a contract awarded by the Directorate of Material of the Royal Netherlands Navy. In the frame of the Implementing Arrangement to the Memorandum of Understanding between the Government of the Kingdom of Sweden and the Minister of Defense of the Kingdom of the Netherlands, NLR has participated in the research program "Smart Skin Array Technologies research".

### VII. REFERENCES

- [1] I.J. Bahl, P. Barthia, *Microstrip Antennas*, Artech House, Dedham (MA), USA, 1980.
- [2] S. Silver, *Microwave Antenna Theory and Design*, Peter Peregrinus, London, UK, 1984.

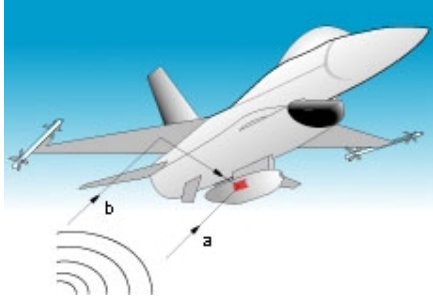


Figure 1 EM interaction between aircraft and conformal antenna array



Figure 2 Conformal antenna array of 16 microstrip patch elements

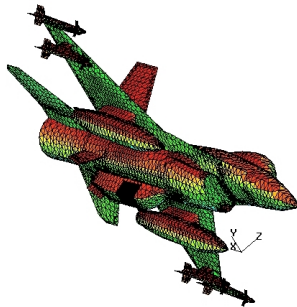


Figure 3 Geometrical approximation of the exterior surface of the aircraft

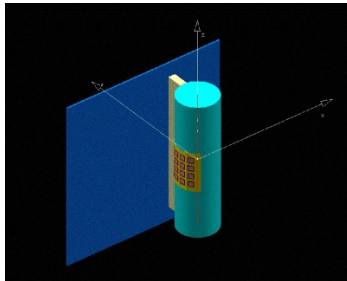


Figure 4 Geometry of the generic aircraft

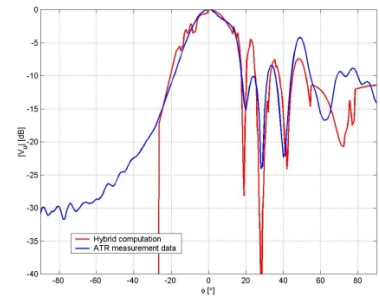


Figure 5 Computational results compared with antenna measurements (horizontal polarisation)

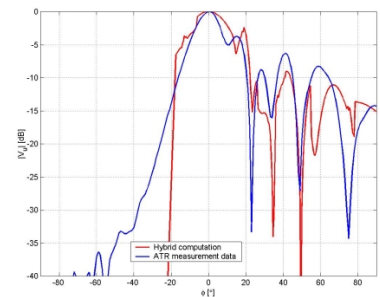


Figure 6 Computational results compared with antenna measurements (vertical polarisation)

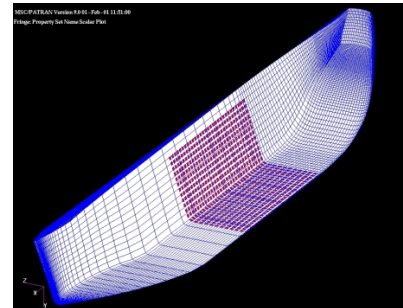


Figure 7 SAR antenna mounted on reconnaissance pod of fighter aircraft

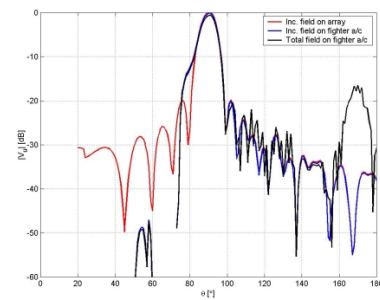


Figure 8 Computational result for SAR antenna on pod